Microwave multiphoton Rabi oscillations

M. Gatzke, M. C. Baruch,* R. B. Watkins, and T. F. Gallagher
Department of Physics, University of Virginia, Charlottesville, Virginia 22901
(Received 17 May 1993)

We have made direct observations of microwave multiphoton Rabi oscillations between two Rydberg states in potassium in the strong-radiation-field regime, where a perturbative treatment of the atom-field interaction becomes invalid. The results of measurements of the Rabi oscillation frequency are presented and compared with results calculated using Floquet theory, which predicts a very different field dependence for the Rabi frequency than is typical in the perturbation-theory limit.

PACS number(s): 32.80.Rm, 32.30.Bv, 42.50.Md

I. INTRODUCTION

During the past several years, experiments with microwaves have demonstrated that resonant multiphoton processes can be driven in Rydberg atoms using field intensities only a fraction of those required for ionization of the atom [1,2]. Most recently, it was shown that the transition amplitudes which result from traversing a multiphoton resonance during the rising and falling edges of a microwave pulse can interfere constructively or destructively leading to interference fringes analogous to those observed using Ramsey's method of separated oscillating fields [3,4]. These experiments confirm that semiclassical Floquet theory can be used to describe the response of a Rydberg atom to an intense pulsed microwave field as an evolution (adiabatic or diabatic) of the atomic Floquet modes, or dressed atomic levels, through avoided-level crossings encountered during the rising and falling microwave field [5]. Although there is little hope of observing these same interference effects using lasers, the issue of diabatic versus adiabatic traversal of dressed-state avoided-level crossings is equally important in high-intensity pulsed-laser experiments [6,7].

Essential for any quantitative description of the evolution of atomic states in the presence of intense radiation is detailed knowledge of the magnitude of the avoided dressed-state level crossings, which are simply the multiphoton Rabi frequencies. Indeed, the Rabi frequency is the fundamental parameter which characterizes the strength of the atom-radiation interaction, and Rabi oscillation, or optical nutation, is the most basic resonant atom-radiation interaction process. Hence measurements of multiphoton Rabi oscillations at nonperturbative intensities, in a system which can be treated with a relatively straightforward semiclassical Floquet model, are especially important for understanding more complicated multiphoton phenomena. It should be noted that microwave multiphoton Rabi oscillations have been observed previously [8,9], but that in these experiments the microwave field intensity was well within the perturbation-theory regime.

In this report we present precise measurements of the Rabi frequency for microwave multiphoton transitions between two bound Rydberg states in potassium (K), made by directly observing Rabi oscillations between the states as a function of time following an initial excitation laser pulse. In the following two sections we briefly introduce the K energy levels under study and review the Floquet theory of multiphoton resonance in this system. Then we describe the experiment in greater detail, present the results of the measurements, and compare them with the predictions of Floquet theory.

II. MICROWAVE MULTIPHOTON TRANSITIONS

All the experiments described in this paper have been done in K using microwave multiphoton transitions between the $21s$ and 19,3 states in combined static and microwave electric fields. The $19,l$ state is the state which is adiabatically connected to the $n = 19$ zero field state of orbital angular momentum l, so that the 19,3 state is adiabatically connected to the $19f$ state at zero field. In Fig. 1 we show an energy-level diagram of the relevant K states of azimuthal orbital angular momentum $m = 0$ and 1 as a function of static electric field. The 19,3 states exhibit a linear Stark shift and the $21s$ state has a small quadratic Stark shift due mostly to Stark mixing with the $21p$ and $20p$ states. As indicated in the inset to Fig. 1, the 19,3 states and the $21s$ state have avoided crossings at fields of 304.2 V/cm for $m = 0$ and 307.9 V/cm for $m = 1$, due to short-range interactions between the Rydberg electron and the K^+ core.

We are interested specifically in the resonant microwave multiphoton transitions which occur from the 21s state to the 19,3 state with $m = 0$, at static fields less than the avoided-crossing field. In Fig. 1 we indicate by arrows the static fields at which the one-, two-, four-, and eight-photon resonances occur for a microwave frequency of 9.1 GHz. The resonances are observed by

*Present address: Imaging Science Technologies, P.O. Box 8175, Charlottesville, VA 22906.

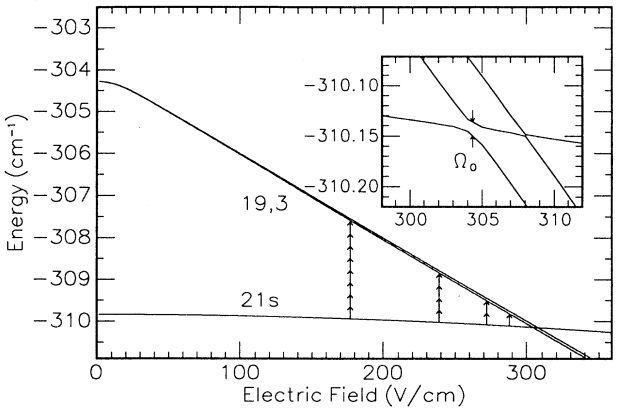

FIG. 1. Energy levels in K near $n = 19$ with $m = 0, 1$ as a function of static electric field. Only the lowest member of the stark manifold (19,3) is shown. The arrows indicate the locations of the one-, two-, four-, and eight-photon resonances at 9.1 GHz. The inset shows the region of the avoided crossings on an expanded scale. Ω_0 is the magnitude of the $m = 0$ avoided crossing.

scanning the static electric field. Initially, atoms are excited to the $21s$ state in the presence of the microwave field, which is then slowly turned off, causing resonant transitions to the 19,3 state [3]. A large electric-field pulse is then applied, ionizing only those atoms which have made the transition [10]. Recording the ion current while scanning the static field produces a series of multiphoton resonances such as those shown in Fig. 2 for a microwave frequency of 9.1 GHz.

The many resonances shown in Fig. 2 illustrate the fact that stronger microwave fields are required to drive the higher-order transitions, which occur at lower static fields. Amid the many resonances, the series of transitions to the 19,3 ($m = 0$) state, marked with arrows separated by about 16 V/cm, is clearly distinguishable. Beginning with the single photon transition at 287 V/cm, the resonances extend to lower field strengths ending with the 18-photon resonance at about 23 V/cm, the highest-order transition observable given our microwave power

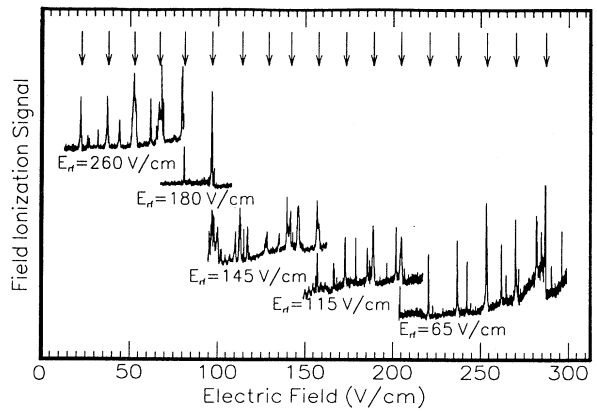

FIG. 2. Microwave multiphoton resonances at 9.1 GHz. The arrows indicate the $21s$-19,3 resonances of 1–18 photons.

limitations. The additional resonances in Fig. 2 correspond to $21s$-19,l transitions, with $l > 3$. Absent from Fig. 2 are resonances involving the 19,3 state with $m = 1$. Despite the polarization of the radiation field along the static field direction, such $\Delta m = 1$ transitions are allowed in our experiment because of the relatively strong spin-orbit coupling in K, evidenced by a small but nonzero avoided crossing of the $21s$ and 19,3 ($m = 1$) states, which is not resolved in the inset of Fig. 1. Nevertheless, our selective field ionization detection method cannot distinguish the signals from these two states, due to the diabatic traversal of their avoided crossing in the rapidly rising ionization field.

III. FLOQUET THEORY OF RESONANCE

Microwave resonance transitions between the 19,3 and $21s$ states can occur whenever atoms initially in one state can absorb or emit an integral number of microwave photons giving them an energy equal to that of the other state. Ignoring for the moment the off-diagonal core coupling between these two states, denoted $\Psi_{19,3}$ and Ψ_{21s}, their energies W in a static field E are

$$W_{19,3} = W_{19,3}(0) - kE,$$
$$W_{21s} = W_{21s}(0) - \frac{\alpha}{2}E^2, \tag{1}$$

where $W_{19,3}(0)/2\pi c = -304.28\ \mathrm{cm}^{-1}$ and $W_{21s}(0)/2\pi c = -309.84\ \mathrm{cm}^{-1}$ are the zero-field binding energies, $k/2\pi = 605\ \mathrm{MHz(V/cm)}^{-1}$ is the electric dipole moment of the 19,3 Stark state, and $\alpha/2\pi = 0.195\ \mathrm{MHz(V/cm)}^{-2}$ is the dipole polarizability of the $21s$ state. In all expressions throughout this paper we will use the convention $\hbar = 1$. In the static field the stationary-state wave functions are

$$\Psi_{19,3}(\mathbf{r}, t) = \Psi_{19,3}(\mathbf{r})e^{-iW_{19,3}t},$$
$$\Psi_{21s}(\mathbf{r}, t) = \Psi_{21s}(\mathbf{r})e^{-iW_{21s}t}. \tag{2}$$

Explicitly assumed in Eq. (2) is that the spatial parts of the wave functions are independent of the field. This approximation ignores both the small admixture of p state into the $21s$ state as well as the nonlinear field dependence of the 19,3 Stark state, evident in Fig. 1, at fields below about 15 V/cm.

If we now add to the static field a radio frequency (rf) field with the same polarization, the total field becomes $E + E_{\mathrm{rf}}\cos(\omega t)$. The addition of the rf field modulates the energy of the 19,3 state about $W_{19,3}(E)$. As first indicated by Townes and Merritt [11], just as modulating the frequency of an optical or radio wave breaks it into a carrier and sidebands, modulating the energy of the 19,3 wave function breaks it into a carrier and sidebands. Accordingly, the 19,3 state can be expressed as a Fourier series in the rf frequency,

$$\Psi_{19,3}(\mathbf{r}, t) = e^{-iW_{19,3}t}\,\Psi_{19,3}(\mathbf{r}) \sum_m J_m\left(\frac{kE_{\mathrm{rf}}}{\omega}\right) e^{im\omega t}, \tag{3}$$

where $J_m(x)$ is the mth-order Bessel function. Similarly, the $21s$ state wave function becomes

$$\Psi_{21s}(\mathbf{r},t) = e^{-i(W_{21s}-\alpha E_{\rm rf}^2/4)t}\,\Psi_{21s}(\mathbf{r})\sum_{n,p} J_{n-2p}\left(\frac{\alpha E E_{\rm rf}}{\omega}\right) J_p\left(\frac{\alpha E_{\rm rf}^2}{8\omega}\right) e^{in\omega t} \tag{4}$$

in the presence of the microwave field [12]. Typically, the static and microwave fields in this experiment satisfy the inequality $8E \gg E_{\rm rf}$. In this case the sidebands of the $21s$ state generated by the *curvature* of its energy as a function of field [represented by the second Bessel function term in Eq. (4)] can be neglected, and the $21s$ wave function can be approximated by

$$\Psi_{21s}(\mathbf{r},t) = e^{-i(W_{21s}-\alpha E_{\rm rf}^2/4)t}\,\Psi_{21s}(\mathbf{r})\sum_{n} J_{n}\left(\frac{\alpha E E_{\rm rf}}{\omega}\right) e^{in\omega t}. \tag{5}$$

A general approach to problems involving Hamiltonians which are periodic in time using Fourier analysis was introduced in 1955 by Autler and Townes [12] and has since become known as Floquet theory [13]. When the Hamiltonian H is time dependent, its eigenstates are not stationary states of single frequency. Still, they resemble stationary states in that they are composed of a single frequency part multiplied by a function periodic in time. Such solutions are often called quasiperiodic. Indeed the quasiperiodic solutions for the wave functions in our system, expressed in Eqs. (3)–(5), have this very specific form, $\Psi(\mathbf{r},t) = \exp(-i\varepsilon t)\Phi(\mathbf{r},t)$, where Φ is periodic in time. In 1965 Shirley [14] showed that the solutions $\Phi(\mathbf{r},t)$ satisfy a *quasi*energy eigenvalue equation $\mathcal{H}\Phi = \varepsilon\Phi$, where $\mathcal{H} = H - i\partial/\partial t$ is called the Floquet Hamiltonian, which, when Fourier expanded, becomes a time-independent matrix eigenvalue equation for $\mathcal{H}$. In fact, this particular separation of the time dependence in the quasiperiodic wave functions is not unique. Equivalently we could use the solution $\Psi(\mathbf{r},t) = \exp[-i(\varepsilon+q\omega)t]\Phi'(\mathbf{r},t)$, where $\Phi' = \exp(iq\omega t)\Phi$ is also periodic and q is any integer. Because of this equivalence there are infinitely many quasienergies (and eigenstates Φ) associated with a particular atomic state Ψ interacting with an oscillating field, all of which are equal modulo the photon energy ω.

In Fig. 3 we show a quasi-energy-level diagram of the 19,3 and $21s$ states as a function of static field. The primary ($q = 0$) $21s$ and 19,3 states are shown as solid lines with an avoided crossing at $E_0 = 304.2$ V/cm, while the broken lines depict the other (dressed state or sideband) quasienergies of the 19,3 state. At specific values of the static field, the multiphoton resonance field E_q, the $21s$ state crosses the qth-order sideband of the 19,3 state. At these values of static field the system exhibits a multiphoton resonance, as described in Sec. II. It is important to note that if the quasienergy states $\Phi_\alpha^{(n)} = \Phi_\alpha \exp(in\omega t)$ are organized according to the magnitude of their quasienergy $\varepsilon_\alpha^{(n)} = W_\alpha + n\omega$, then the Floquet Hamiltonian matrix elements $(\omega/2\pi)\int_0^{2\pi/\omega} dt\langle\Phi_\alpha^{(n)}|\mathcal{H}_F|\Phi_\beta^{(m)}\rangle$ will be not only diagonal but also (2×2) block degenerate at the resonances. Here the labels α and β represent either $21s$ or 19,3.

In the solutions for the wave functions in Eqs. (3) and (5), and in the quasienergy plot of Fig. 3, we have ignored the off-diagonal core coupling. When it is included, each of the quasi-energy-level crossings of Fig. 3 becomes an avoided crossing, similar to the one in a purely static field E_0. In the static case, the level separation Ω_0 at the avoided crossing is

$$\Omega_0 = 2\langle\Psi_{21s}(\mathbf{r})|H_C|\Psi_{19,3}(\mathbf{r})\rangle, \tag{6}$$

where H_C is the off-diagonal part of the core coupling Hamiltonian. Including this coupling in the Floquet Hamiltonian with the rf field present lifts the degeneracy of the quasienergies at the multiphoton resonances. Treating the coupling as a perturbation to our Floquet quasienergy eigenvalue problem will therefore require an application of degenerate perturbation theory. In fact, if the resonances are distinct and not overlapping, then to a very good approximation the (2×2) blocks may be diagonalized independently, permitting a nearly exact solution for the quasi-energy-level separations near a resonance. Because the Hamiltonian H_C is time independent, in Shirley's Floquet theory the matrix elements in each degenerate block couple only the time-independent Fourier components of the scalar product of the two wave functions,

$$\frac{\omega}{2\pi}\int_0^{\frac{2\pi}{\omega}} dt\langle\Phi_{21s}^{(p)}(\mathbf{r},t)|H_C|\Phi_{19,3}^{(p-q)}\mathbf{r},t)\rangle = \frac{\Omega_0}{2}\sum_{m,n} J_m\left(\frac{kE_{\rm rf}}{\omega}\right) J_n\left(\frac{\alpha E E_{\rm rf}}{\omega}\right)\frac{\omega}{2\pi}\int_0^{\frac{2\pi}{\omega}} dt\, e^{i[(m+p-q)-(n+p)]\omega t}$$

$$= \frac{\Omega_0}{2}\sum_{n} J_{n+q}\left(\frac{kE_{\rm rf}}{\omega}\right) J_n\left(\frac{\alpha E E_{\rm rf}}{\omega}\right), \tag{7}$$

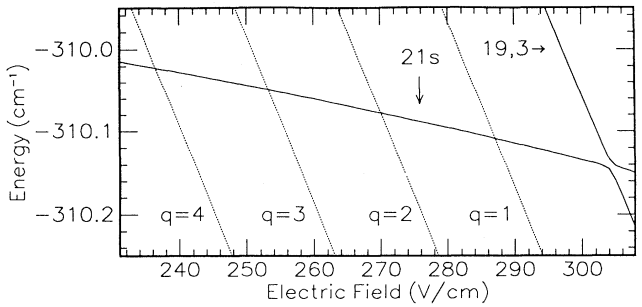

FIG. 3. Quasi-energy-level diagram as a function of static electric field, with zero rf field amplitude.

where the last relation results from the orthogonality of the Fourier expansion functions. The double summation can be further simplified [15] so that the resonant quasi-energy-level or dressed-state avoided crossings are

$$\Omega_q \equiv 2\left[\frac{\omega}{2\pi}\int_0^{\frac{2\pi}{\omega}} dt\langle\Phi_{21s}^{(p)}(\mathbf{r},t)|H_C|\Phi_{19,3}^{(p-q)}(\mathbf{r},t)\rangle\right] = \Omega_0 J_q\left(\frac{(k-\alpha E)E_{\mathrm{rf}}}{\omega}\right). \tag{8}$$

Note that this result is independent of p so that each dressed-state avoided crossing is equivalent. Floquet theory has therefore reduced our multiphoton resonance problem to a simple static two-state system involving only the original $21s$ and 19,3 states coupled by the interaction expressed in Eq. (8).

Solving the two-state problem using standard techniques produces solutions which exhibit quantum beats, when prepared in the appropriate initial state. These quantum beats, or oscillations, between two orthogonal superpositions of the nearly degenerate dressed states are simply resonant Rabi oscillations, or optical nutations [16]. If atoms are excited initially to one of the states ($21s$), at some later time t there is an oscillating probability $P(t)$ of finding the atoms in the other state (19,3). Explicitly,

$$P(t) = \frac{|\Omega_q|}{\sqrt{\Delta_q^2+\Omega_q^2}}\sin^2\left(\frac{(\Omega_q^2+\Delta_q^2)^{\frac{1}{2}}t}{2}\right), \tag{9}$$

where Ω_q is called the q-photon-resonance Rabi frequency, and

$$\Delta_q = W_{19,3} - W_{21s} - q\omega \simeq (k-\alpha E_q)(E_q - E) \tag{10}$$

is the detuning from resonance. At resonance ($\Delta_q = 0$), Eq. (9) reduces to

$$P(t) = \sin^2\left(\frac{\Omega_q t}{2}\right) = \frac{1}{2}[1-\cos(\Omega_q t)], \tag{11}$$

and the probability oscillates in time between the resonant $21s$ and 19,3 states with frequency Ω_q. There is, in principle, an alternative approach to observing resonance. If the $21s$ state is initially excited at a static field far from a resonance and the levels are then tuned through the resonance by rapidly sweeping the static field, the transition probability to the 19,3 state is predicted by the Landau-Zener formula [17],

$$P(t) = 1 - \exp\left[-\frac{\pi\Omega_q^2}{2\dot{\Delta}}\right], \tag{12}$$

where

$$\dot{\Delta} = \frac{d\Delta}{dt} \simeq -(k-\alpha E_q)\frac{dE}{dt} \tag{13}$$

is the sweep rate of the detuning. By observing the Landau-Zener transition probability $P(t)$ as a function of the sweep rate $\dot{\Delta}$, the Rabi frequency can be determined using Eq. (12). In practice we found that this method did not yield results as reliable as those obtained by directly observing Rabi oscillations. In fact, the transition probability observed was not exponential in time, as predicted by Eq. (12), but instead exhibited evident substructure, possibly associated with the traversal of other resonances during the sweep of the detuning.

Before leaving this section we emphasize the fact that our Floquet analysis of multiphoton resonance has required a high-frequency approximation,

$$\Omega_q < \Omega_0 \ll \omega, \tag{14}$$

ensuring that the resonances be distinct and well resolved. For the states we have chosen this requires an rf frequency greater than 1 GHz. At lower frequencies a similar treatment must include the contributions from several neighboring, nearly degenerate quasienergy states simultaneously, which would tend to shift and broaden the resonances.

IV. EXPERIMENTAL APPROACH

In order to observe the multiphoton resonances and accurately measure their Rabi frequencies, we require a system which can produce large pulsed microwave fields, high voltage ionizing fields, and tunable homogeneous static electric fields. As demonstrated by Stoneman, Thomson, and Gallagher, a resonant microwave cavity constructed by closing the ends of a piece of waveguide can produce microwave fields large enough to observe resonances involving more than 20 photons [1]. By including inside their cavity a copper septum placed perpendicular to the microwave field and insulated from the waveguide, they could also create both the ionizing and tunable static electric fields required. In fact, the apparatus we used is essentially the same as the one used by Stoneman, Thomson, and Gallagher, with a few significant improvements. In particular, the microwave cavity has been enlarged to improve the field homogeneity. The new cavity is a piece of WR 229 (S band) waveguide 8.32 cm long, closed at both ends. The inside dimensions are 2.92 × 5.80 × 8.32 cm. There are 1.0 mm diameter holes in two of the cavity's sidewalls to admit the atomic

and laser beams, and there is a 0.3 mm diameter hole in the center of the top of the waveguide to allow ions to escape. The septum is a copper plate 3.1 mm thick supported by insulating Teflon supports in the four corners of the cavity. The cavity itself is dc insulated from the rest of the vacuum system so that it can be biased as well. The distance from the septum to the top of the waveguide is 7.36 mm. The center of the atomic beam passes approximately midway between the septum and the top of the cavity. With this arrangement we are able to obtain a field homogeneity of 0.007% over the region of detection, almost two orders of magnitude better than the previous experiment.

The cavity was operated in the TE_{105} mode near 9.26 GHz. With the septum in place the mode structure of the empty cavity is altered slightly, with several different resonances associated with this mode occurring at slightly lower frequencies. The cavity's time constant of 28 ns resulted in a quality factor Q of about 1600. Microwave power is coupled into the cavity using a coaxial probe inserted from the bottom of the cavity. Maximal coupling is achieved by adjusting the length of the probe. For some of the measurements the cavity was *over*coupled, which reduced its time constant to only 8 ns. The microwave power originates in a Hewlett-Packard (HP) 8350B sweep oscillator with an HP 83550A X band plug-in. After passing through a mixer used to pulse modulate the microwaves, the pulses are amplified in a Hughes 1277H traveling-wave-tube amplifier. The amplified microwave pulses are attenuated and then traverse a waveguide, a four-port dual-directional coupler, and a semirigid coaxial cable before reaching the cavity. A dc-blocking capacitor is used to isolate the ground of the coaxial cable from the cavity. The directional coupler allows for measurement of both the incident and reflected microwave powers using an HP 432A power meter. With this arrangement we estimate that we can determine the microwave field inside the cavity to within $\simeq 15\%$.

The experiment is performed inside a vacuum chamber with a background gas pressure of less than 10^{-6} Torr. A beam of K atoms from a resistively heated source enters the microwave cavity through the hole in one sidewall. Light from two pulsed dye laser beams tuned to the $4s$-$4p$ and $4p$-$21s$ transitions in K enters the identical hole on the opposite sidewall and is focused at the center of the cavity where atoms are exited to the $21s$ state. The light is polarized along the electric-field direction so that only the $m = 0$ states can be excited. The rf pulse is applied to the cavity about 300 ns before the arrival of the laser pulses to ensure that the microwave field has reached its steady state when the $21s$ atoms are created. The falling edge of the rf pulse is followed in several hundred ns by a high voltage field ionization pulse applied to the septum in the cavity. The precise voltage and rise time of this pulse are chosen so as to ionize only atoms in the 19,3 state, not those in the $21s$ state [10]. The voltage pulse required is about 2.2 kV, with a typical rise time of 1 μs. The ions from atoms directly under the 0.3 mm hole in the top of the cavity then accelerate in the ionizing field are ejected from the cavity and impinge upon the microchannel plate particle multiplier

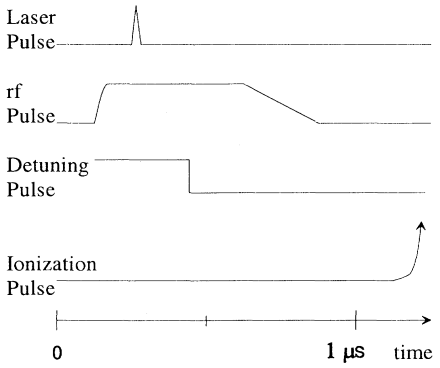

FIG. 4. Experimental timing scheme.

above the cavity. In addition to the ionizing field pulse from the septum, a small, rapidly rising field pulse produced by applying voltage pulses to the cavity can be used to detune the atoms from resonance in the time between the laser pulse and the falling edge of the rf field pulse. Figure 4 summarizes the basic timing scheme used in the experiment.

Rabi oscillations are observed directly by fixing the static field exactly on resonance and applying a ($\simeq 1$ V) negative voltage detuning pulse to the cavity, delayed some fixed time from the laser pulses. This detuning pulse is generated with a HP 8112A programmable pulse generator with a rise time of 4.5 ns, whose delay time is computer controlled through a GPIB interface. By stepping the delay of this pulse between laser shots, the time the atoms spend in resonance can be scanned as the 19,3 field ionization signal is recorded, producing Rabi oscillation signals such as those shown in Fig. 5. Here the delay step time was 1 ns, and the signal at a given delay was averaged over many laser shots to increase the signal to noise ratio. This method of rapid Stark detuning of the levels from resonance to generate Rabi oscillations was also used in previous measurements [8,9] and is similar to the one used by Brewer and Shoemaker who were the first to observe optical nutation in molecular resonances using

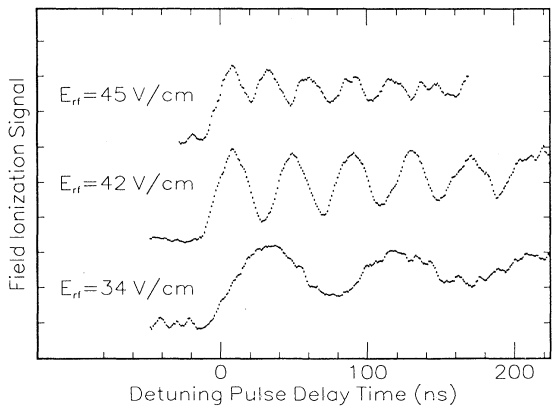

FIG. 5. Rabi oscillation signals for the four photon resonance.

CO_2 laser radiation [18]. A similar technique has also been used to generate quantum beats between Rydberg states at level crossings in static electric fields [19].

V. RESULTS AND DISCUSSION

We have observed Rabi oscillations such as those illustrated in Fig. 5 for a selected subset of the $21s$-19,3 multiphoton resonances shown in Fig. 2 at many different rf field strengths. By fitting the observed signals to a sinusoidal oscillation for positive laser-detuning pulse delay times, the Rabi frequency can be determined with great accuracy, typically to within 2%. The results are shown as a function of rf field for the one-, two-, and four-photon resonances in Fig. 6(a) and for the 8-, 13-, and 18-photon resonances in Fig. 6(b). The solid curves in the figures indicate the predictions of Floquet theory expressed in Eq. (8). Here we use a value for the static field avoided crossing of $\Omega_0 = 323$ MHz, which was calculated from a direct solution of the energy eigenvalue problem for a K atom in an electric field using measured values for the quantum defects [20]. This value for Ω_0 is also consistent with previous measurements [21].

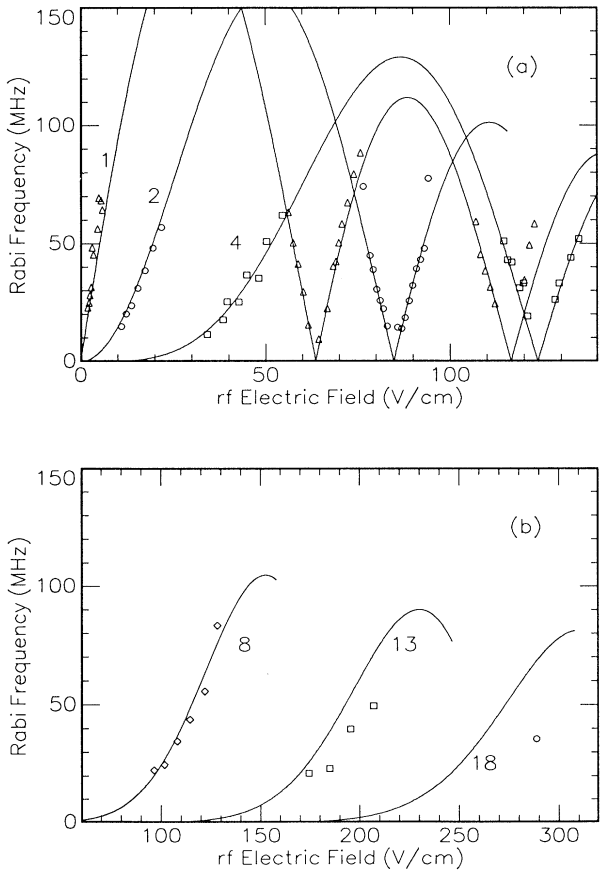

FIG. 6. Measured Rabi oscillation frequencies for (a) the one-, two, and four-photon resonances and (b) the 8-, 13-, and 18-photon resonances. As mentioned in the text, the rf field amplitudes of the data in (a) have been scaled (lower by 15% on average) to provide best fits to the calculated results.

The agreement between the measurements and the predictions of Floquet theory is remarkable for the lower-order resonances, extending over a great range of both static and rf fields. Furthermore, it is important to note that, unlike previous work [8,9], our experiment includes results for the strong-field regime, where perturbation theory does not apply. Our measurements therefore strongly support the validity of this nonperturbative Floquet treatment of resonance. For the 13- and 18-photon resonances, there appears to be a systematic disagreement between the calculations and the measurements. In fact, the simple two state model we used in Sec. III should be expected to break down in these cases. This is because our calculations have ignored other states in the Stark manifold which are coupled at zero field, and the total field certainly passes through zero during measurements involving these resonances.

Aside from the striking agreement between theory and experiment, the most notable feature of Fig. 6 is that, for particular values of the rf field strength, the Rabi frequency of a given multiphoton transition vanishes. This occurs for the same reason that sidebands in the power spectrum of a frequency modulated sine wave vanish at certain modulation amplitudes. A nearly identical effect was also observed in the transverse optical pumping experiments which first demonstrated the effectiveness of the dressed-state approach to problems involving atoms in rf fields [22]. While a more detailed theoretical treatment predicts that the Rabi frequencies actually pass continuously through zero, from positive to negative values, our experiment is not sensitive to the sign (or orientation) of the Rabi nutation. We can determine only the magnitude of the nutation frequency through the expression in Eq. (9) for the transition probability.

Another noteworthy feature of Fig. 6 is the limited frequency range of the measurements. Rabi oscillations of frequency greater than about 70 MHz are impossible to generate with our current approach due to the finite width of the laser pulse. Upon excitation at a multiphoton resonance, atoms are created in a superposition of the two energy eigenstates, which then oscillates between the $21s$ and 19,3 states. The finite time of the laser pulse produces atoms with a distribution of different starting times for the oscillation. The net signal is then an average over starting time or, equivalently, over a range of phases. With a very long Rabi oscillation period, this range of phases is small and the effect is insignificant. However, as the oscillation period becomes comparable to the laser-pulse width, the phase average begins to decrease the amplitude of the oscillation. The observed upper limit of our Rabi oscillation frequency gives an estimate of 5–10 ns for the dye laser-pulse width, in good agreement with its measured value of 10 ns.

In addition to an upper limit for the measurements presented in Fig. 6, there is a less apparent lower limit as well, caused by the presence of inhomogeneity in the applied electric fields. In general, field inhomogeneity results in a damping of the observed Rabi oscillations. One reason for the damping is simply the inhomogeneous distribution of detunings from resonance [Δ_q of Eq. (10)]

produced by the spatial inhomogeneity in the static field E and the finite volume of the laser foci. However, averaging the oscillation expressed in Eq. (11) over detunings produces a relatively slow damping. In fact, for Rabi frequencies much smaller than the nominal inhomogeneous detuning, the damped oscillations closely resemble a Bessel function, which damps as $t^{-1/2}$. Such slow damping does not pose a limitation to the experiment if the signal to noise ratio is sufficient to overcome the overall loss of oscillation amplitude which also results. The observation of many oscillations is then still possible, providing for an accurate determination of the Rabi frequency.

The type of damping just discussed is often referred to as inhomogeneous damping and must be distinguished from the inherent relaxation of the oscillation process which results from atomic motion in the presence of the field inhomogeneity [23]. It is this relaxation damping which ultimately determines the lower limit of the Rabi frequencies we are able to observe. Because the atoms in the atomic beam have a finite velocity of roughly 0.4 mm/μs, they move through the region of detection in less than 1 μs. In the presence of a static field inhomogeneity, they are effectively shifted into and out of resonance as they move through the cavity. Even a very small field inhomogeneity of $\delta E/E = 0.01\%$ results in a comparably large distribution of detunings $\Delta_q = (k - \alpha E_q)\delta E \simeq 16$ MHz for the lower-order resonances. Atoms whose Rabi frequencies are less than this will be shifted into and out of resonance in less than 1 μs, setting an upper limit on the time over which Rabi oscillations may be observed. Requiring at least two complete oscillations for an adequate fit of the frequency sets a lower limit of about 10 MHz for our measurements. Of course, a much more sophisticated approach can be applied to determine the actual time dependence of relaxation damping. However, without detailed knowledge of the inhomogeneous field distribution, such a quantitative analysis is unwarranted.

An rf field inhomogeneity can also present a problem for observing Rabi oscillations. This is especially true for measurements made near the zero crossings, i.e., near the zeros of the Bessel function which determines the Rabi frequency's dependence on rf field strength in Eq. (8). We estimate that, because of the cavity's mode structure, the rf field is inhomogeneous at the level of a few percent over the region of detection. Near a zero crossing this can result in a distribution of Rabi frequencies over a range of about 5 MHz, which would damp a 10 MHz oscillation in about one cycle. In general, such estimates are consistent with the observation that damping is more severe near the zero crossings than for measurements at much lower rf fields, suggesting that the rf inhomogeneity dominates in these cases.

All damping effects have been accounted for empirically in our analysis by including an exponential decay rate factor $e^{-t/\tau}$ in our fit to the oscillations. In those cases in which many oscillations are observed, the inclusion of such a factor had an effect of only a few percent on the result for the oscillation frequency. Typically, the rate constant τ which best fit the data was greater than 100 ns, again suggesting 10 MHz as a lower limit for our measurements.

Although we can measure the Rabi frequencies with great accuracy, a similar level of accuracy is not possible for the calibration of the applied rf field. Indeed, the largest uncertainty in many microwave experiments including this one is the determination of the microwave field strength. In this experiment the sensitivity of the Rabi frequency to the rf field near the zero crossing is extreme. Consequently, rf field calibration error presents an unusually difficult problem when comparing our measurements with the calculated results of Sec. III. What follows is a description of our treatment of this problem.

The data presented in Fig. 6 were collected during runs on many different days, each run lasting several hours. At the beginning and end of each run, the rf field was calibrated against a microwave ionization threshold in the K atom (see Ref. [24] for experimental details) so that data of different runs could be matched together. The run to run variance in the measurements of this threshold field was only 3.7%. However, the overall systematic uncertainty in the measurement is dominated by the estimated microwave power measurement uncertainty of 15%. In particular, our result for the calibration of the microwave ionization threshold field for the $28d$ ($m = 0$) state at 9.1 GHz is $110 \pm 4 \pm 16$ V/cm.

In addition, the rf field can be calibrated by observing the small shift of the resonance associated with the ac Stark shift of the $21s$ state, $\Delta W_{\rm ac} = \alpha E_{\rm rf}^2/4$, where α is the polarizability of the $21s$ state defined in Eq. (1) [1]. We have measured these shifts for both the one- and four-photon resonances, obtaining a calibrated ionization threshold field for the $28d$ ($m = 0$) state of $115 \pm 3 \pm 2$ V/cm. The systematic error is small because the resonance fields can be measured very accurately. However, this calibration depends on the assumption that the ac Stark shift of the $21s$ state is simply its time averaged shift in the presence of the rf field, which may not be valid at the level of a few percent. Nevertheless, this calibration is in agreement with the original microwave power calibration and therefore provides a check of our power measurements.

Therefore, while the precision of the relative rf field calibration for all the measurements is good, the absolute field calibration contains a rather large systematic uncertainty. As a result, the data presented in Fig. 6(a) have been scaled to provide a best fit to the theory. The rf electric fields for these data have been multiplied by the factors 0.81, 0.87, and 0.87 for the one-, two-, and four-photon resonances, respectively, suggesting a systematic error in the absolute rf field calibration of 15% and a 4% relative uncertainty. Therefore, these scalings are consistent with both the estimated rf power measurement uncertainty and the run to run scatter of the threshold measurements. The data of Fig. 6(b), which are not as sensitive to the rf field calibration, have all been scaled by 0.85, the average scaling factor from the data in Fig. 6(a). As a final note, we conclude that, given a sufficient level of confidence in the Floquet calculations of Sec. III, our Rabi frequency measurements can provide a calibration of the microwave field amplitude which is

far more accurate than possible with techniques which involve power measurements in the microwave system.

VI. CONCLUSION

Our measurements have clearly demonstrated that the two-level Floquet model of Sec. III accurately describes resonant microwave multiphoton transitions between the K $(n+2)s$ states and n, k Stark states in combined static and microwave fields. As a consequence, one can use the calculated Floquet quasienergy modes, or dressed levels, and their avoided crossings to determine the response of this system to pulsed microwave radiation in future experiments.

ACKNOWLEDGEMENT

This work has been generously supported by the Air Force Office of Scientific Research.

[1] R.C. Stoneman, D.S. Thomson, and T.F. Gallagher, Phys. Rev. A **37**, 1527 (1988).
[2] W. van de Water *et al.*, Phys. Rev. Lett. **63**, 762 (1989); Phys. Rev. A **42**, 572 (1990).
[3] M.C. Baruch and T.F. Gallagher, Phys. Rev. Lett. **68**, 3515 (1992).
[4] S. Yoakum, L. Sirko, and P.M. Koch, Phys. Rev. Lett. **69**, 1919 (1992).
[5] H.P. Breuer, K. Dietz, and M. Holthaus, Z. Phys. D **8**, 349 (1988); **10**, 13 (1988).
[6] D.G. Papaioannou and T.F. Gallagher, Phys. Rev. Lett. **69**, 3161 (1992).
[7] J.G. Story, D.I. Duncan, and T.F. Gallagher, Phys. Rev. Lett. **70**, 3012 (1993).
[8] T.R. Gentile, B.J. Hughey, D. Kleppner, and T.W. Ducas, Phys. Rev. A **40**, 5103 (1989).
[9] L. Sirko, A. Buchleitner, and H. Walther, Opt. Commun. **78**, 403 (1990).
[10] T.F. Gallagher and W.E. Cooke, Phys. Rev. A **19**, 694 (1979); T.F. Gallagher *et al.*, *ibid.* **16**, 1098 (1977).
[11] C.H. Townes and F.R. Merritt, Phys. Rev. **72**, 1266 (1947).
[12] S.H. Autler and C.H. Townes, Phys. Rev. **100**, 703 (1955).
[13] S.-I. Chu, Adv. At. Mol. Phys. **21**, 197 (1985).
[14] J.H. Shirley, Phys. Rev. **138B**, 979 (1965).
[15] *Handbook of Mathematical Functions*, Natl. Bur. Stand. Appl. Math. Ser. No. 55, edited by M. Abramowitz and I. A. Stegun (U.S. GPO, Washington, DC, 1964).
[16] L. Allen and J.H. Eberly, *Optical Resonance and Two-Level Atoms* (Wiley, New York, 1975).
[17] L.D. Landau and E.M. Lifshitz, *Quantum Mechanics: Non-Relativistic Theory*, 3rd ed. (Pergamon, New York, 1977), p. 350.
[18] R.G. Brewer and R.L. Shoemaker, Phys. Rev. Lett. **27**, 631 (1971).
[19] G. Leuchs and H. Walther, Z. Phys. A **293**, 93 (1979); T.H. Jeys *et al.*, Phys. Rev. A **23**, 3065 (1981).
[20] M.L. Zimmerman *et al.*, Phys. Rev. A **20**, 2251 (1979).
[21] R.C. Stoneman, G. Janik, and T.F. Gallagher, Phys Rev. A **34**, 2952 (1986).
[22] C. Cohen-Tannoudji, *Cargèse Lectures in Physics* (Gordon and Breach, New York, 1968), Vol. 2, p. 347.
[23] H.C. Torrey, Phys. Rev. **104**, 563 (1956); G.D. Cates *et al.*, Phys. Rev. A **38**, 5209 (1988).
[24] H.B. van Linden van den Heuvell and T.F. Gallagher, Phys Rev. A **32**, 1495 (1985); P. Pillet *et al.*, *ibid.* **30**, 280 (1984).